AIAA JOURNAL
Vol. 48, No. 6, June 2010

Interval Analysis Method for Damage Identification of Structures

Xiaojun Wang,* Haifeng Yang, and Zhiping Qiu
Beijing University of Aeronautics and Astronautics, 100191 Beijing, People's Republic of China

DOI: 10.2514/1.45325

Based on the availability of measured natural frequencies of structures, the interval analysis technique was proposed for structural damage identification. Influences of uncertainties in the measurements and modeling errors on the identification were investigated. Because of the lack of information on measurement uncertainties, the interval description was adopted for the measured natural frequencies in this paper. Via the first-order Taylor series expansion, the interval bounds of the elemental stiffness parameters of both undamaged and damaged structures were derived by using the model updating based on the initial analytical finite element model. The damage can be identified by comparing the differences between the two models, where the quantitative measure of the possibility of damage existence in the elements is introduced. A larger value of possibility of damage existence implied a higher possibility of damage occurrence. The damage identifications for a steel cantilever beam and a steel cantilever plate were performed by the presented method, which is validated by Monte Carlo simulation. Moreover, the case of the multidamage identification, the number of the used natural frequencies, and the effects of damage level and uncertainty level on the damage detection were studied as well. The numerical results proved the validity and applicability of the presented interval analysis method.

Nomenclature

$\boldsymbol{b}$, (b_i)	=	uncertain parameters
$\boldsymbol{b}^c$	=	center of uncertain parameter
$\boldsymbol{b}^I$	=	interval of uncertain parameter
$d\boldsymbol{K}$, $d\lambda_i$, $d\boldsymbol{\phi}_i$	=	change quantities for $\boldsymbol{K}$, λ_i, and $\boldsymbol{\phi}_i$
$d\boldsymbol{\alpha}$	=	elemental stiffness change
$\bar{d}\boldsymbol{\alpha}(\boldsymbol{b})$	=	upper bound for $d\alpha$
$\underline{d}\boldsymbol{\alpha}(\boldsymbol{b})$	=	lower bound for $d\alpha$
$d\boldsymbol{\alpha}^I(\boldsymbol{b})$	=	interval of stiffness change
$d\lambda$	=	eigenvalue change
$\boldsymbol{K}$	=	stiffness matrix in unchanged state
$\boldsymbol{K}_c$	=	stiffness matrix in changed state
$\boldsymbol{K}_i$	=	elemental parameterized stiffness matrix
$\boldsymbol{M}$	=	mass matrix in unchanged state
$\boldsymbol{M}_c$	=	mass matrix in change state
$p(\cdot)$	=	probably density function
p_d^i	=	probability of damage existence
p_i	=	possibility of damage existence
$\boldsymbol{S}$	=	eigensensitivity matrix
$(X_i)_j$	=	realization of random variable
$\boldsymbol{\alpha}_c$, (α_{ci})	=	elemental stiffness parameters in changed state
α_i	=	ith elemental stiffness parameter
$\boldsymbol{\alpha}_d^I$, (α_{di}^I)	=	damaged parameter intervals
$\boldsymbol{\alpha}_r^I$, (α_{ri}^I)	=	undamaged parameter intervals
$\Delta\boldsymbol{b}$, (Δb_i)	=	maximum uncertainty of parameters
$\Delta\boldsymbol{b}^I$	=	uncertain interval of parameter
$\delta\boldsymbol{b}$, (δb_i)	=	variable quantities of b
$\underline{\lambda}_c$, $(\underline{\lambda}_{ci})$	=	lower bounds of eigenvalue
$\bar{\lambda}_c$, $(\bar{\lambda}_{ci})$	=	upper bounds of eigenvalue
λ_i, λ_{ci}	=	ith eigenvalue, unchanged and changed
λ_c^I, (λ_{ci}^I)	=	eigenvalue intervals
$\boldsymbol{\phi}_i$, $\boldsymbol{\phi}_{ci}$	=	ith eigenvector, unchanged and changed
$\Omega(\alpha_{di})$	=	damaged parameter distribution
$\Omega(\alpha_{ri})$	=	undamaged parameter distribution

Received 7 May 2009; revision received 29 January 2010; accepted for publication 31 March 2010. Copyright © 2010 by the American Institute of Aeronautics and Astronautics, Inc. All rights reserved. Copies of this paper may be made for personal or internal use, on condition that the copier pay the $10.00 per-copy fee to the Copyright Clearance Center, Inc., 222 Rosewood Drive, Danvers, MA 01923; include the code 0001-1452/10 and $10.00 in correspondence with the CCC.

*Institute of Solid Mechanics; XJWang@buaa.edu.cn.

I. Introduction

VARIOUS types of damages of engineering structures are often reported in civil, mechanical, and aerospace engineering fields. These damages maybe due to overloading, corrosion, material aging, or other unexpected events, and they could cause the structure to work ineffectively, leading to possible failure. During the last two decades, the vibration-based structural damage identification methods have been developed extensively. It is based on the fact that local damages usually cause a decrease in the structural stiffness, which will change the global vibration characteristics of the structure.

Vibration data used for damage detection include natural frequency, mode shape, mode shape curvature, modal flexibility, and modal strain energy. Abo [1] used the information of the change of natural frequencies and mode shapes to identify structural damage. A damage identification method using mode shape sensitivities to the changes in mass or stiffness in the test structure was presented in literature [2]. Robinson et al. [3] proposed a method for detecting structural damage in an aircraft fuselage using the dynamically measured flexibility matrix. Additionally, some hybrid methods have also been developed by other researchers [4,5]. Model updating is an important method in damage detection. In this method, a theoretical finite element (FE) model of a structure is adjusted to the updated model which is consistent with dynamic measured data. The sensitivity-based FE model updating method using experimental modal data was used for structural damage identification [6,7], and an eigenstructure assignment approach of model updating was applied in the literature [8,9].

However, an inherent problem exists in the model updating method. There is a difference between the actual response of the structure and the theoretical response predicted by the analytical model due to the various unavoidable uncertainties. Many damage identification methods assume that the initial analytical FE model is identical to the structure and the measurements are accurate. In practice, however, modeling errors arising from the assumptions and simplifications made in the modeling process exist, as well as the noise of the data measured from the vibration tests. Such uncertainties in the analysis process may result in fault results of the damage identification. Therefore, it is very important to develop an effective method to solve the problem of structural damage identification *with* uncertainties. At present, there are mainly three methods for solving uncertain problems [10]: namely, probabilistic analysis approach, fuzzy analysis method, and set-based theoretical

convex method. In the analysis of uncertain structural damage identification, the probabilistic analysis method, and fuzzy analysis method have been widely used [11–13] and obtained some satisfying results. The Monte Carlo simulation technique is the most straightforward and popular tool in probabilistic methods, but the calculation is time-consuming. Moreover, the precondition of applying the probabilistic approach is that the probability density function (PDF) of uncertain variables is known. However, in most cases, it is hard to determine the probability density function due to the complexity of the sources of uncertainties and lack of sufficient experimental data. Hence, most literature assumes that the uncertain variables obey a certain probability distribution. However, such an assumption may lead to questionable results. In the fuzzy analysis method, a fuzzy variable is defined as a member of the fuzzy subset of a domain. Like the PDF in the probabilistic analysis approach, the membership function is defined to describe the degree of membership to this fuzzy subset of each element in the domain. It is clear that the most serious problem in the two methods is the impossibility of obtaining an exact probability density function or exact membership function to describe the practical uncertain variables.

Set-based theoretical convex methods, including convex models [14] and interval analysis [15,16], are the effective *nonprobabilistic* methods to deal with the uncertain problems [17]. The interval analysis method has been applied in multiple engineering fields [18,19]. In this method, the uncertain quantities are considered as interval numbers rather than random or fuzzy variables. Compared to probabilistic and fuzzy analysis approaches, the interval analysis method requires less information: namely, only the bounds of the uncertain parameters, which could easily be obtained in practical engineering problems. Gabriele et al. [20] combined the model updating and interval analysis to develop an interval damage identification method. García et al. [21] proposed a new methodology based on the combination of interval analysis and constraint propagation techniques and applied it to the structural assessment of the Sorraia River Bridge.

In this paper, an interval method for the damage identification of structures is proposed based on Taylor series expansion [22] and model updating theory [6,23].

II. Sensitivity-Based FE Model Updating Procedure for Interval Damage Identification

Consider the free vibration problem of an undamped structure with N degrees of freedom:

$$\boldsymbol{M}\ddot{\boldsymbol{x}}(t) + \boldsymbol{K}\boldsymbol{x}(t) = 0 \tag{1}$$

where $\boldsymbol{M}$ is the $N \times N$ mass matrix, $\boldsymbol{K}$ is the $N \times N$ stiffness matrix, and $\boldsymbol{x}(t)$ and $\ddot{\boldsymbol{x}}(t)$ are the displacement and acceleration vectors, respectively. The eigenvalue problem corresponding to Eq. (1) can be expressed as [23]

$$\boldsymbol{K}\boldsymbol{\phi}_i = \lambda_i \boldsymbol{M}\boldsymbol{\phi}_i, \qquad i = 1, 2, \ldots, N \tag{2}$$

where λ_i and $\boldsymbol{\phi}_i$ are the ith eigenvalue and mass-normalized mode shape, respectively. If there are changes in the structural parameters due to modeling errors or structural damage, the eigenvalue problem can be written as

$$\boldsymbol{K}_c\boldsymbol{\phi}_{ci} = \lambda_{ci}\boldsymbol{M}_c\boldsymbol{\phi}_{ci}, \qquad i = 1, 2, \ldots, N \tag{3}$$

where $\boldsymbol{K}_c$, $\boldsymbol{M}_c$, λ_{ci}, and $\boldsymbol{\phi}_{ci}$ are the mass matrix, stiffness matrix, ith eigenvalue and mass-normalized mode shape, respectively, in the changed state. Because of the structural damage, we suppose that changes occur in $\boldsymbol{K}$, λ_i and $\boldsymbol{\phi}_i$, whereas the mass $\boldsymbol{M}$ remains unchanged. They can be expressed as

$$\begin{aligned} \boldsymbol{K}_c &= \boldsymbol{K} + d\boldsymbol{K}, \qquad \boldsymbol{M}_c = \boldsymbol{M} \\ \lambda_{ci} &= \lambda_i + d\lambda_i, \qquad \boldsymbol{\phi}_{ci} = \boldsymbol{\phi}_i + d\boldsymbol{\phi}_i \end{aligned} \tag{4}$$

where $d\boldsymbol{K}$, $d\lambda_i$, and $d\boldsymbol{\phi}_i$ denote the respective change in the stiffness matrix, the eigenvalue, and eigenvector.

Substituting Eq. (4) into Eq. (3) and left-multiplying $\boldsymbol{\phi}_i^T$, the following expression can be obtained by neglecting the high-order terms:

$$\boldsymbol{\phi}_i^T \cdot d\boldsymbol{K} \cdot \boldsymbol{\phi}_i = d\lambda_i = \lambda_{ci} - \lambda_i \tag{5}$$

For the FE model of a structure, the matrix $\boldsymbol{K}$ can be expressed in the following form of nonnegative parameter decomposition:

$$\boldsymbol{K} = \sum_{i=1}^{m} \alpha_i \boldsymbol{K}_i = \alpha_1 \boldsymbol{K}_1 + \alpha_2 \boldsymbol{K}_2 + \ldots + \alpha_m \boldsymbol{K}_m \tag{6}$$

where m is the number of elements in the structure, α_i is initial elemental stiffness parameter (bending stiffness in this paper), and $\boldsymbol{K}_i$ is the ith elemental stiffness matrix divided by α_i. Similarly, the matrix $\boldsymbol{K}_c$ in the changed state is obtained as

$$\boldsymbol{K}_c = \sum_{i=1}^{m} \alpha_{ci} \boldsymbol{K}_i = \alpha_{c1} \boldsymbol{K}_1 + \alpha_{c2} \boldsymbol{K}_2 + \ldots + \alpha_{cm} \boldsymbol{K}_m \tag{7}$$

According to Eqs. (6) and (7), Eq. (5) can be rewritten as follows:

$$\boldsymbol{\phi}_i^T \left(\sum_{j=1}^{m} (\alpha_{cj} - \alpha_j) \boldsymbol{K}_j \right) \boldsymbol{\phi}_i = \boldsymbol{\phi}_i^T \left(\sum_{j=1}^{m} d\alpha_j \boldsymbol{K}_j \right) \boldsymbol{\phi}_i = d\lambda_i \tag{8}$$

Furthermore, Eq. (8) can be written as [23]

$$\boldsymbol{S} \cdot d\boldsymbol{\alpha} = d\boldsymbol{\lambda} \tag{9}$$

where $d\boldsymbol{\alpha}$ and $d\boldsymbol{\lambda}$ are the elemental stiffness change vector and eigenvalue change vector, respectively; $\boldsymbol{S}$ is the eigensensitivity matrix whose elements are

$$S_{ij} = \boldsymbol{\phi}_i^T \boldsymbol{K}_j \boldsymbol{\phi}_i, \qquad i = 1, 2, \ldots, n, \qquad j = 1, 2, \ldots, m \tag{10}$$

where n is the number of available measured frequencies. If n equals the number of the elements in structure, m, then $\boldsymbol{S}$ will be a square matrix. In practice, n is usually less than m. Thus the problem becomes indeterminate with an infinite amount of solutions. Generally, its solution can be written as [23,24]

$$d\boldsymbol{\alpha} = \boldsymbol{S}^+ \cdot d\boldsymbol{\lambda} \tag{11}$$

where $\boldsymbol{S}^+$ is the Moore–Penrose generalized inverse of matrix $\boldsymbol{S}$. So $d\boldsymbol{\alpha}$ could be obtained from Eq. (11). Since Eq. (5) was derived by neglecting high-order terms, a procedure of iterative computation should be carried out to reduce error due to the first-order approximation, which can be described as follows:

Step 1) Solve Eq. (2) at the $(p+1)$th iteration with the known $\boldsymbol{\alpha}^{(p)}$ for λ_i and $\boldsymbol{\phi}_i$.

Step 2) Solve Eq. (10) at the $(p+1)$th iteration with the known $\boldsymbol{\alpha}^{(p)}$ for $\boldsymbol{S}$.

Step 3) Solve Eq. (11) at the $(p+1)$th iteration with the known $\boldsymbol{\alpha}^{(p)}$ and the computed $\boldsymbol{S}$ for $d\boldsymbol{\alpha}^{(p+1)}$.

Step 4) Update the stiffness parameter vector by the formula

$$\boldsymbol{\alpha}^{(p+1)} = \boldsymbol{\alpha}^{(p)} + d\boldsymbol{\alpha}^{(p+1)} \tag{12}$$

Step 5) Repeat the iterative procedures until the following criterion is satisfied:

$$\frac{|\boldsymbol{\alpha}_c^{(p+1)} - \boldsymbol{\alpha}_c^{(p)}|}{|\boldsymbol{\alpha}_c^{(p+1)}|} < 1.0 \times 10^{-6} \tag{13}$$

It should be stressed that the formulas above were discussed without considering the effect of uncertainties on the damage identification. In the following sections, interval-based parameter identification and damage identification of structures with uncertain measurements will be given.

III. Interval Identification of the Elemental Stiffness Parameter

It is very possible that if the uncertainty level is larger than or close to the frequency changes due to damages, the damaged members cannot be identified and in some cases the healthy members may be identified as damaged. In this paper, the parameter errors of modeling can be reduced by a two-step model updating procedure which will be introduced in the next section. In each model updating procedure, the measurement uncertainties are considered as the main factors affecting the damage identification results. This takes place due to the fact that the updated elemental stiffness parameters are more sensitive to the measurement uncertainties than the FE modeling errors [23]. Based on interval mathematics, the eigenvalue intervals with uncertainty in the changed state can be expressed as

$$\begin{aligned} \boldsymbol{\lambda}_c^I &= [\underline{\boldsymbol{\lambda}}_c, \overline{\boldsymbol{\lambda}_c}] = (\lambda_{c1}^I, \lambda_{c2}^I, \ldots, \lambda_{cn}^I)^T \\ \lambda_{ci}^I &= [\underline{\lambda}_{ci}, \overline{\lambda_{ci}}], \qquad i = 1, 2, \ldots, n \end{aligned} \tag{14}$$

where $\underline{\boldsymbol{\lambda}}_c$ and $\underline{\lambda}_{ci}$ are the lower bounds of the eigenvalue vector and components; $\overline{\boldsymbol{\lambda}_c}$ and $\overline{\lambda_{ci}}$ are the upper bounds of the eigenvalue vector and components. The middle value and the radius (or uncertainty) of an interval number or vector are introduced [17]:

$$\boldsymbol{x}^c = m(\boldsymbol{x}^I) = \frac{\underline{\boldsymbol{x}} + \bar{\boldsymbol{x}}}{2} \tag{15}$$

$$\Delta \boldsymbol{x} = \mathrm{rad}(\boldsymbol{x}^I) = \frac{\bar{\boldsymbol{x}} - \underline{\boldsymbol{x}}}{2} \tag{16}$$

where $\boldsymbol{x}^c$ and $\Delta \boldsymbol{x}$ are the middle value and the radius (or uncertainty) of $\boldsymbol{x}^I$, respectively. Therefore, the uncertain measured parameters (referred to as the measured natural frequencies in this study) in the undamaged or damaged state of the structure can be rewritten in the following form

$$\begin{aligned} \boldsymbol{b}^I &= \boldsymbol{b}^c + \Delta \boldsymbol{b}^I = \boldsymbol{b}^c + \Delta \boldsymbol{b}[-1, 1] = \boldsymbol{b}^c + \Delta \boldsymbol{b} e_\Delta \\ \boldsymbol{b}^c &= (b_1^c, b_2^c, \ldots, b_n^c)^T, \qquad \Delta \boldsymbol{b} = (\Delta b_1, \Delta b_2, \ldots, \Delta b_n)^T \end{aligned} \tag{17}$$

where $e_\Delta = [-1, 1]$, and the superscript c and script Δ represent the corresponding middle value and the radius of the interval numbers or vector, respectively.

Consider the damage identification formula, Eq. (9). The vectors $d\boldsymbol{\alpha}$ and $d\boldsymbol{\lambda}$ and the matrix $\boldsymbol{S}$ are the functions of $\boldsymbol{b} = (b_1, b_2, \ldots, b_n)^T$, so they can be written as

$$d\boldsymbol{\alpha} = d\boldsymbol{\alpha}(\boldsymbol{b}) = (d\alpha_1(\boldsymbol{b}), d\alpha_2(\boldsymbol{b}), \ldots, d\alpha_m(\boldsymbol{b}))^T \tag{18}$$

$$d\boldsymbol{\lambda} = d\boldsymbol{\lambda}(\boldsymbol{b}) = (d\lambda_1(\boldsymbol{b}), d\lambda_2(\boldsymbol{b}), \ldots, d\lambda_n(\boldsymbol{b}))^T \tag{19}$$

$$\boldsymbol{S} = \boldsymbol{S}(\boldsymbol{b}) = (S_{ij}(\boldsymbol{b}))_{n \times m} \tag{20}$$

Based on the interval expression, Eq. (17), the vector $\boldsymbol{b}$ can be expressed in the following form:

$$\begin{cases} \boldsymbol{b} = \boldsymbol{b}^c + d\boldsymbol{b}, & |d\boldsymbol{b}| < \Delta \boldsymbol{b} \\ b_i = b_i^c + db_i, & |db_i| < \Delta b_i, \qquad i = 1, 2, \ldots, n \end{cases} \tag{21}$$

If we expand Eqs. (18–20) as the first-order Taylor series in terms of db_i, we get

$$d\boldsymbol{\alpha}(\boldsymbol{b}) = d\boldsymbol{\alpha}(\boldsymbol{b}^c + d\boldsymbol{b}) \approx d\boldsymbol{\alpha}(\boldsymbol{b}^c) + \sum_{i=1}^{n} \frac{\partial (d\boldsymbol{\alpha}(\boldsymbol{b}^c))}{\partial b_i} db_i \tag{22}$$

$$d\boldsymbol{\lambda}(\boldsymbol{b}) = d\boldsymbol{\lambda}(\boldsymbol{b}^c + d\boldsymbol{b}) \approx d\boldsymbol{\lambda}(\boldsymbol{b}^c) + \sum_{i=1}^{n} \frac{\partial (d\boldsymbol{\lambda}(\boldsymbol{b}^c))}{\partial b_i} db_i \tag{23}$$

$$\boldsymbol{S}(\boldsymbol{b}) = \boldsymbol{S}(\boldsymbol{b}^c + \delta \boldsymbol{b}) \approx \boldsymbol{S}(\boldsymbol{b}^c) + \sum_{i=1}^{n} \frac{\partial \boldsymbol{S}(\boldsymbol{b}^c)}{\partial b_i} db_i \tag{24}$$

Substituting Eqs. (22–24) into Eq. (9) and neglecting high-order terms, the following equations can be obtained:

$$d\boldsymbol{\alpha}(\boldsymbol{b}^c) = \boldsymbol{S}(\boldsymbol{b}^c)^+ \cdot d\boldsymbol{\lambda}(\boldsymbol{b}^c) \tag{25}$$

$$\begin{aligned} &\sum_{i=1}^{n} \frac{\partial (d\boldsymbol{\alpha}(\boldsymbol{b}^c))}{\partial b_i} db_i \\ &\quad = \boldsymbol{S}(\boldsymbol{b}^c)^+ \sum_{i=1}^{n} \left(\frac{\partial (d\boldsymbol{\lambda}(\boldsymbol{b}^c))}{\partial b_i} - \frac{\partial \boldsymbol{S}(\boldsymbol{b}^c)}{\partial b_i} \cdot d\boldsymbol{\alpha}(\boldsymbol{b}^c) \right) db_i \end{aligned} \tag{26}$$

where $db_i \in \Delta b_i^I = [-\Delta b_i, \Delta b_i]$. Substitution of Eqs. (25) and (26) into Eq. (22), leads to the expression for $d\boldsymbol{\alpha}$:

$$\begin{aligned} d\boldsymbol{\alpha}(\boldsymbol{b}) &= \boldsymbol{S}(\boldsymbol{b}^c)^+ \cdot d\boldsymbol{\lambda}(\boldsymbol{b}^c) \\ &\quad + \boldsymbol{S}(\boldsymbol{b}^c)^+ \sum_{i=1}^{n} \left(\frac{\partial (d\boldsymbol{\lambda}(\boldsymbol{b}^c))}{\partial b_i} - \frac{\partial \boldsymbol{S}(\boldsymbol{b}^c)}{\partial b_i} \cdot d\boldsymbol{\alpha}(\boldsymbol{b}^c) \right) db_i \end{aligned} \tag{27}$$

Using the natural interval extension, we can obtain the change interval of the elemental stiffness:

$$\begin{aligned} d\boldsymbol{\alpha}^I(\boldsymbol{b}) &= \boldsymbol{S}(\boldsymbol{b}^c)^+ \cdot d\boldsymbol{\lambda}(\boldsymbol{b}^c) \\ &\quad + \sum_{i=1}^{n} \boldsymbol{S}(\boldsymbol{b}^c)^+ \left(\frac{\partial (d\boldsymbol{\lambda}(\boldsymbol{b}^c))}{\partial b_i} - \frac{\partial \boldsymbol{S}(\boldsymbol{b}^c)}{\partial b_i} \cdot d\boldsymbol{\alpha}(\boldsymbol{b}^c) \right) \cdot \Delta b_i^I \end{aligned} \tag{28}$$

Since $\Delta b_i^I = \Delta b_i [-1, 1]$, the lower and upper bounds of the interval vector $d\boldsymbol{\alpha}^I$ will be

$$\begin{aligned} \underline{d\boldsymbol{\alpha}(\boldsymbol{b})} &= \boldsymbol{S}(\boldsymbol{b}^c)^+ \cdot d\boldsymbol{\lambda}(\boldsymbol{b}^c) \\ &\quad - \sum_{i=1}^{n} \left| \boldsymbol{S}(\boldsymbol{b}^c)^+ \left(\frac{\partial (d\boldsymbol{\lambda}(\boldsymbol{b}^c))}{\partial b_i} - \frac{\partial \boldsymbol{S}(\boldsymbol{b}^c)}{\partial b_i} \cdot d\boldsymbol{\alpha}(\boldsymbol{b}^c) \right) \right| \cdot \Delta b_i \end{aligned} \tag{29}$$

$$\begin{aligned} \overline{d\boldsymbol{\alpha}(\boldsymbol{b})} &= \boldsymbol{S}(\boldsymbol{b}^c)^+ \cdot d\boldsymbol{\lambda}(\boldsymbol{b}^c) \\ &\quad + \sum_{i=1}^{n} \left| \boldsymbol{S}(\boldsymbol{b}^c)^+ \left(\frac{\partial (d\boldsymbol{\lambda}(\boldsymbol{b}^c))}{\partial b_i} - \frac{\partial \boldsymbol{S}(\boldsymbol{b}^c)}{\partial b_i} \cdot d\boldsymbol{\alpha}(\boldsymbol{b}^c) \right) \right| \cdot \Delta b_i \end{aligned} \tag{30}$$

The interval radius vector $\Delta(d\boldsymbol{\alpha})$ is not updated iteratively since the iterative process may lead to the enhancement of the interval radii of $d\boldsymbol{\alpha}^I$. Thus, the lower and upper bounds of $d\boldsymbol{\alpha}^I$ can be obtained from Eqs. (12), (13), (29), and (30). The sensitivity coefficients $\partial (d\boldsymbol{\lambda}(\boldsymbol{b}^c))/\partial b_i$ and $\partial \boldsymbol{S}(\boldsymbol{b}^c)/\partial b_i$ can be obtained according to the following equations:

$$\begin{aligned} \frac{\partial (d\lambda_j(\boldsymbol{b}^c))}{\partial b_i} &= \frac{\partial \lambda_{cj}(\boldsymbol{b}^c)}{\partial b_i} - \frac{\partial \lambda_j(\boldsymbol{b}^c)}{\partial b_i}, \\ i &= 1, 2, \ldots, n, \qquad j = 1, 2, \ldots, n \end{aligned} \tag{31}$$

$$\begin{aligned} \frac{\partial S_{jk}(\boldsymbol{b}^c)}{\partial b_i} &= \frac{\partial (\boldsymbol{\phi}_j(\boldsymbol{b}^c)^T \boldsymbol{K}_k \boldsymbol{\phi}_j(\boldsymbol{b}^c))}{\partial b_i} = 2\boldsymbol{\phi}_j(\boldsymbol{b}^c)^T \boldsymbol{K}_k \frac{\partial \boldsymbol{\phi}_j(\boldsymbol{b}^c)}{\partial b_i} \\ i &= 1, 2, \ldots, n, \qquad j = 1, 2, \ldots, n, \qquad k = 1, 2, \ldots, m \end{aligned} \tag{32}$$

For the initial analytical FE model, it is clear that λ_j and $\boldsymbol{\phi}_j$ are independent of measured parameters. Hence,

$$\frac{\partial \lambda_j(\boldsymbol{b}^c)}{\partial b_i} = 0, \qquad \frac{\partial \boldsymbol{\phi}_j(\boldsymbol{b}^c)}{\partial b_i} = 0, \qquad \frac{\partial \lambda_{cj}}{\partial b_i} = 1 \tag{33}$$

Substituting Eqs. (31–33) into Eqs. (29) and (30), the lower and upper bounds of interval vector $d\boldsymbol{\alpha}^I$ in the changed state can be determined. In other words, the undamaged and damaged FE models can be updated by the uncertain measured eigenvalues and the initial analytical FE model, respectively. In the next step, the damage in the structure can be identified by comparing the undamaged and damaged FE models.

IV. Possibility of Damage Existence

Applying the model updating method for interval parameter identification developed in previous sections, the elemental stiffness parameter vectors within the undamaged and damaged FE models can be obtained as two interval vectors:

$$\boldsymbol{\alpha}_r^I = (\alpha_{r1}^I, \alpha_{r2}^I, \ldots, \alpha_{ri}^I, \ldots, \alpha_{rm}^I)^T, \qquad i = 1, 2, \ldots, m \tag{34}$$

$$\boldsymbol{\alpha}_d^I = (\alpha_{d1}^I, \alpha_{d2}^I, \ldots, \alpha_{di}^I, \ldots, \alpha_{dm}^I)^T, \qquad i = 1, 2, \ldots, m \tag{35}$$

The structural damage can be identified easily through the comparison of these two vectors when α_{ri} and α_{di} are real numbers. Nevertheless, due to uncertainty, the real elemental stiffness parameters α_{ri} and α_{di} will fall into the intervals denoted here as $[\underline{\alpha_{ri}}, \overline{\alpha_{ri}}]$ and $[\underline{\alpha_{di}}, \overline{\alpha_{di}}]$, respectively. For interval numbers $[\underline{\alpha_{ri}}, \overline{\alpha_{ri}}]$ and $[\underline{\alpha_{di}}, \overline{\alpha_{di}}]$, we cannot directly identify the damage of structures. Generally, the middle value of α_{di}^I is less than the middle value of α_{ri}^I. It cannot be assured, however, that the value of α_{ri} will always be larger than the value of α_{di}. To address this problem, the elemental stiffness parameters of the undamaged and damaged FE models (α_{di}^I and α_{ri}^I) are represented on the same axis, as shown in Fig. 1. The quantitative measure of the possibility of damage existence (PoDE) can be introduced. The two rectangles in Fig. 1 represent the region of variations of α_{ri} and α_{di}. The interval of α_{ri}^I obtained by the first model updating procedure represents the healthy interval for the ith element. The hatched region denotes the possible damaged region. The PoDE in the elements denoted as p_i can be defined as

$$p_i = \frac{\overline{\alpha_{ri}} - \underline{\alpha_{di}}}{\overline{\alpha_{di}} - \underline{\alpha_{di}}} \times 100\% \tag{36}$$

where p_i takes a value between 0 and 100%. If the damage in an element does not take place or the lower bound of α_{ri}^I is equal to or less than the lower bound of α_{di}^I, p_i will vanish. On the other hand, if the value of p_i for an element is 100%, we conclude that the upper bound of α_{di}^I is equal to or less than the lower bound of α_{ri}^I; in other words, damage with a certain degree exists in the element.

V. Monte Carlo Simulation for Damage Identification of Structures

In the probability approach, the measured natural frequencies in undamaged and damaged states are considered as uncertain random variables. To apply the Monte Carlo technique to the structural damage identification, the probability distributions for the random variables are needed. The normal distribution is often chosen because of its simplicity in analysis, but it may not be appropriate for practical circumstances because these variables are generally located within certain intervals. To model this fact the truncated normal distribution $p(x_i)$ is introduced for random variable x_i:

$$p(x_i) = \begin{cases} C_i \exp\left(-\frac{x_i^2}{B_i^2}\right), & |x_i| \le A_i \\ 0, & |x_i| > A_i \end{cases} \tag{37}$$

where $p(x_i)$ is the probability density function of x_i, A_i is the maximum possible value for random variable x_i, B_i is the parameter determining the curve shape, and C_i is the normalization constant:

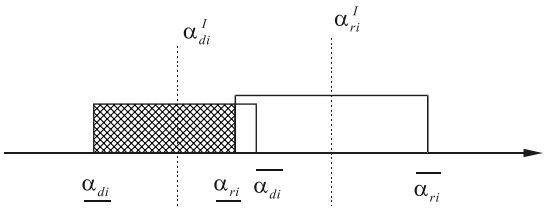

Fig. 1 Scheme for the comparison of α_{ri} and α_{di}.

$$C_i = \left[2B_i \cdot \operatorname{erf}\left(\frac{A_i}{B_i}\right)\right]^{-1} \tag{38}$$

where the error function $\operatorname{erf}(\cdot)$ is defined as

$$\operatorname{erf}(x) = \int_0^x e^{-t^2}\, dt \tag{39}$$

Here, it is assumed that the random variables are independent of each other. The probability density functions of x with various values of B are shown in Fig. 2. It is clear that a lager B corresponds to a more dispersive distribution. When $B^2 \ll A^2$, the variable x_i is nearly uniformly distributed. The realizations of x_i, denoted by $(X_i)_j$ $(j = 1, 2, \ldots)$ can be generated by the formula

$$(X_i)_j = B_i \cdot \operatorname{erf}^{-1}\left[(2\delta_j - 1) \cdot \operatorname{erf}\left(\frac{A_i}{B_i}\right)\right] \tag{40}$$

where δ_j $(j = 1, 2, \ldots)$ are independent random numbers uniformly distributed in [0,1].

Once the samples of truncated normal distributed random variables are obtained, Monte Carlo simulations can be carried out to obtain the probability density function of elemental stiffness parameters in both undamaged and damaged states based on Eq. (11). They are distributed in intervals $\Omega(\alpha_{ri})$ and $\Omega(\alpha_{di})$, as illustrated in Fig. 3. The probability of damage existence (PrDE) is defined as [6,23]

$$p_d^i = \operatorname{prob}(L_{di} < x_{\alpha_{di}} \le L_{ri}) = 1 - \operatorname{prob}(L_{ri} \le x_{\alpha_{di}} < U_{di}) \tag{41}$$

where L_{di} and U_{di} are the lower and upper bounds of $\Omega(\alpha_{di})$, respectively, and L_{ri} and U_{ri} are the lower and upper bounds of $\Omega(\alpha_{ri})$, respectively. A higher PrDE value implies more likelihood

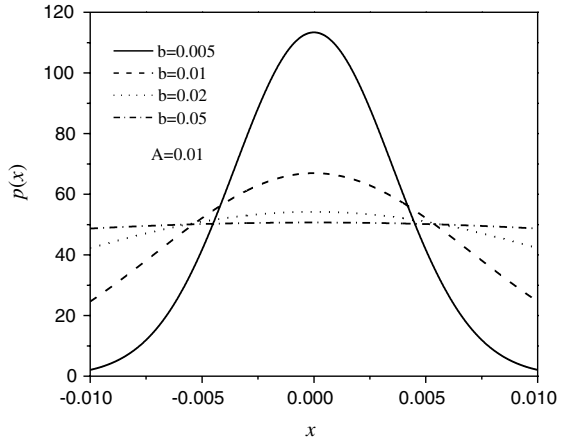

Fig. 2 Probability density function for a truncated normally distributed random variable.

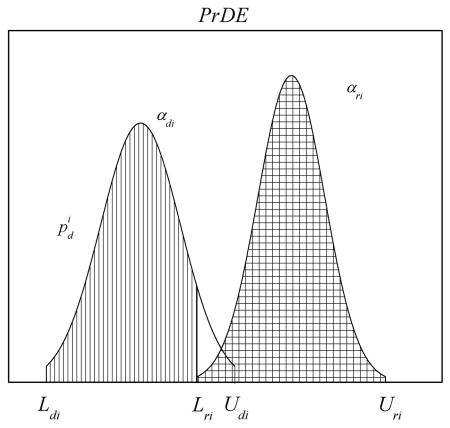

Fig. 3 Probability density functions of α_{ci}, α_i, and PrDE.

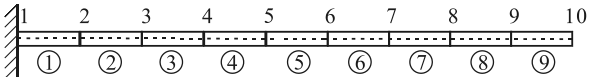

Fig. 4 FE model of the cantilever beam.

for damage. On the contrary, if the PrDE value is close to zero, we could conclude that the element is more likely to be healthy.

VI. Numerical Examples

A. Example I

To illustrate the validity of the present interval method for damage identification, a steel cantilever beam [23] with 9 Euler-Bernoulli elements ($m = 9$) and 10 nodes was used (Fig. 4). The cross section of the beam is rectangular, with an area of 50.75×6 mm^2. The length of each element is 100 mm. The mass density of the material is 7.67×10^3 kg/m^3, and the actual Young's modulus in the intact state is 2.0×10^{11} N/m^2. Suppose that the elemental stiffness parameters (bending stiffness) of the initial analytical model are 1.1 times larger than that of the undamaged model, and the damaged model is the same as the undamaged model except that the bending stiffness is reduced by 20% in element 5. The elemental bending stiffnesses of initial model, undamaged model, and damaged model are $\alpha_{I1\text{–}9} = 200.97$ Nm^2, $\alpha_{r1\text{–}9} = 182.7$ Nm^2, $\alpha_{d1\text{–}4,6\text{–}9} = 182.7$ Nm^2, and $\alpha_{d5} = 0.8 \times \alpha_{d1\text{–}4,6\text{–}9} = 146.16$ Nm^2, respectively. The first six natural frequencies ($n = 6$) of the three models are listed in Table 1, and the natural frequencies of undamaged and damaged models are assumed to be uncertain measured parameters b_i.

1. *Comparison with Monte Carlo Simulation*

Both of the uncertain measured natural frequencies in undamaged and damaged state are interval numbers. The associated uncertain radii are equal to 1% of the corresponding middle values. Therefore,

$$\lambda_i^I = [0.99\lambda_i^c, 1.01\lambda_i^c], \qquad i = 1, 2, \ldots, 6 \tag{42}$$

For the comparison with the probabilistic method, it is also assumed that these uncertain quantities have the truncated normal distributions within the given intervals, which can be expressed as the mean values plus the random noises:

$$\lambda_{ci} = \lambda_{ci}^0(1 + X_i) \tag{43}$$

Table 1 Natural frequencies of the three models (in hertz)

	Natural frequency					
Model	1	2	3	4	5	6
Initial model	6.41	40.14	112.44	220.56	365.44	548.18
Undamaged model	6.11	38.27	107.20	210.30	348.44	522.67
Damaged model	6.04	36.63	106.95	202.82	345.60	508.21

where λ_{ci}^0 is the mean value of the ith measured eigenvalue and X_i is the truncated normal distributed random noise, which can be generated by Eq. (40).

In the first updating procedure, the initial FE model was updated to obtain the undamaged FE model using the uncertain measured natural frequencies in undamaged state of the structure. The middle values and the lower and upper bounds of the elemental stiffness parameters in the undamaged state obtained by the interval analysis method are listed in Table 2. To verify the results, the Monte Carlo technique was also carried out. The maximum possible value A_i of X_i is set as 1%, corresponding to Eq. (42). Parameter B_i is fixed at 0.1, which means that the variable X_i is nearly uniform. The results of 40,000 simulations are listed in Table 2. We found that the lower bounds of elemental stiffness parameters obtained by the proposed method were slightly smaller than that obtained by the Monte Carlo method. Further, the upper bounds of elemental stiffness parameters obtained by the interval method were slightly larger than that obtained by the Monte Carlo method. The middle values obtained by the interval analysis method were nearly equal to the mean values obtained by Monte Carlo simulation. Moreover, both of them were very close to the true value. However, due to the lack of natural frequency information (only the first six natural frequencies are available), the middle values obtained by interval analysis and Monte Carlo simulation cannot converge to the true values.

The second FE model updating procedure was carried out to obtain the elemental stiffness parameters of the damaged FE model based on the initial analytical FE model and the uncertain measured natural frequencies in the damaged state. Again, both the interval analysis method and Monte Carlo technique were used. The middle values and the lower and upper bounds of the elemental stiffness parameters are listed in Table 3. The results are very similar to that of the undamaged FE model, the intervals of the elemental stiffness parameters obtained by interval method were slightly wider than those obtained by Monte Carlo technique, and their middle values were again very close (but not equal) to the true values.

Based on the undamaged and damaged FE models obtained above, the damage in elements can be identified by comparing the differences between the two models. The values of PoDE for all elements according to Eq. (36) are listed in Table 4, and the values of PrDE for all elements obtained by the Monte Carlo technique are also listed in Table 4. As shown in Table 4, element 5 has 100% PoDE as well as PrDE. Element 1 has 14.58% PoDE. This is caused by the error coming from first-order Taylor series expansion and the uncertainties of measured natural frequencies in undamaged and damaged states. For the Monte Carlo simulation, the PrDE of element 1 is 1.7%, which is much smaller than 14.58% obtained by the interval method. Comparing to Monte Carlo simulation, the interval analysis method is more conservative. This is because of the insufficient information about the distribution of uncertain parameters and the interval extension of interval mathematics. However, the interval method is more efficient in computation than Monte Carlo simulation, the execution time of the interval method is only 10% of the probabilistic method. In practice, both 1.7 and 14.58% would indicate the low possibility of damage for element 1.

Table 2 Mean values and bounds of elemental stiffness parameters in undamaged state (in Nm^2)

		Mean value			Lower bound		Upper bound	
Element number	True value	Interval method	Error level of interval method	Monte Carlo method	Interval method	Monte Carlo method	Interval method	Monte Carlo method
1	182.7	183.38	0.37%	183.34	165.47	167.36	201.29	199.33
2	182.7	182.70	0.00%	182.70	169.35	170.87	196.06	194.54
3	182.7	181.28	0.78%	181.32	157.27	160.28	205.28	202.35
4	182.7	182.85	0.08%	182.87	171.02	172.06	194.69	193.67
5	182.7	182.35	0.19%	182.40	163.63	166.71	201.06	198.10
6	182.7	181.86	0.46%	181.89	165.47	167.51	198.26	196.26
7	182.7	183.54	0.46%	183.54	171.74	173.09	195.34	193.98
8	182.7	182.89	0.10%	182.81	153.46	156.23	212.31	209.38
9	182.7	183.72	0.56%	183.85	139.31	142.20	228.12	225.50

Table 3 Mean values and bounds of elemental stiffness parameters in damaged state (in Nm^2)

Element number	True value	Mean value			Lower bound		Upper bound	
		Interval method	Error level of interval method	Monte Carlo method	Interval method	Monte Carlo method	Interval method	Monte Carlo method
1	182.7	177.73	2.72%	177.68	160.42	162.29	195.04	193.06
2	182.7	184.23	0.84%	184.25	171.21	172.79	197.25	195.70
3	182.7	187.18	2.45%	187.24	163.92	166.49	210.43	207.99
4	182.7	186.97	2.34%	187.00	175.53	176.70	198.42	197.29
5	146.2	143.60	1.78%	143.57	125.38	128.20	161.81	158.94
6	182.7	181.22	0.81%	181.24	165.37	167.43	197.07	195.05
7	182.7	182.77	0.04%	182.77	171.15	172.35	194.40	193.19
8	182.7	179.56	1.72%	179.49	151.18	153.61	207.94	205.37
9	182.7	182.65	0.03%	182.79	139.87	143.23	225.42	222.35

Table 4 PoDEs and PrDEs of the elements

Element number	PoDE, %	PrDE, %[a]
1	14.58	1.70
2	0.00	0.00
3	0.00	0.00
4	0.00	0.00
5	100	100
6	0.34	0.00
7	2.53	0.05
8	4.02	0.10
9	0.00	0.00

[a]$A_i = 0.01$ and $B_i = 0.1$.

From the above discussion, it can be concluded that the interval damage identification method can provide effective results with limited information of uncertainties. The damage detection results were verified by Monte Carlo simulation. When the parameter information is limited or the probability distribution densities of uncertainties are unknown, the probabilistic method cannot be used effectively. At this time, the interval analysis method can prove to be supplementary to the probabilistic damage identification.

2. Multidamage Identification

In practice, there tends to be more than one damaged region in a structure. Thus, an effective damage identification method should have the ability to detect multiple regions of damage. In this section, the multidamage identification will be carried out based on the present interval analysis method. Structures with two damaged elements out of a total of nine elements will be studied. The damage identification results are listed in Table 5. In the first case the elements 5 and 7 are damaged (20% reduction of bending stiffness). Remarkably, the two elements are identified to have a 100% possibility being damaged. Elements 1, 3, 6, and 8 have lower possibilities of damage existence. Their PoDEs are 21.41, 12.89, 10.45, and 16.12%, respectively. Other elements have little possibility of damage. In another case, element 1 and element 5 are considered to be damaged (20% reduction of bending stiffness). Each of their PoDEs is identified as 100%. The PoDEs of element 2 and element 6 are 28.02 and 7.12%, respectively. The PoDEs for some undamaged elements are increased a small degree in the interval multidamage identification.

3. Interval Damage Identification Using Different Numbers of Natural Frequencies

The first six natural frequencies were used to detect damages in a cantilever beam in previous sections. In this section, different numbers of natural frequencies will be used for detecting damage of the structure. The damage identification results by the first five natural frequencies and the first seven natural frequencies are listed in Table 6. When the five natural frequencies are used, the damage element is identified accurately. However, the PoDEs of healthy elements increase. Obviously, this may lead to a false detection. On the contrary, if the number of natural frequencies used increases to seven, the PoDEs of the healthy elements will decrease; the PoDE of the damaged element decreases too. It can be concluded that the number of natural frequencies used for damage detection has some effect on the PoDEs of all the elements, but the damage can also be detected.

4. Study on Damage Level

The damage levels of elements that indicate the reduction degree of bending stiffness in this paper have a great effect on the results of damage detection of structures. A higher level of damage can be identified more easily. On the other hand, if the damage level is very low, the false results may be obtained due to the effect of uncertain measurements, since the true information is submerged in noise. Numerical analyses were performed with different structural damage levels to study the effect of damage level on the damage identification results. We assume that the interval radii of uncertain parameters equal to 1% and the different damage levels in element 5 are 10, 20, and 30%, respectively; namely, the bending stiffness of element 5 are 164.43 Nm^2, 146.16 Nm^2 and 127.89 Nm^2, respectively. The mean

Table 5 PoDEs of elements for different multidamage identifications

Element number	PoDE, %		
	20% reduction of bending stiffness in element 5	20% reduction of bending stiffness in elements 5, 7	20% reduction of bending stiffness in elements 1, 5
1	14.58	21.41	100
2	0.00	0.00	28.02
3	0.00	12.89	0.00
4	0.00	0.00	2.40
5	100	100	100
6	0.34	10.45	7.12
7	2.53	100	3.10
8	4.02	16.12	0.00
9	0.00	0.00	0.00

Table 6 PoDEs of elements using different number of natural frequencies

Element number	PoDE, %		
	Using the first six natural frequencies	Using the first five natural frequencies	Using the first seven natural frequencies
1	14.58	38.51	4.08
2	0.00	0.00	0.00
3	0.00	0.00	0.00
4	0.00	0.00	2.27
5	100	100	82.58
6	0.34	0.45	0.00
7	2.53	2.96	0.00
8	4.02	15.90	3.26
9	0.00	0.00	4.49

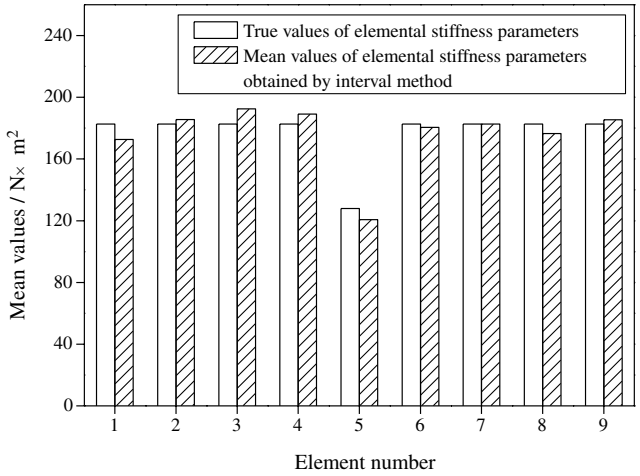

Fig. 5 Mean values of elemental stiffness parameters at the damage level of 30%.

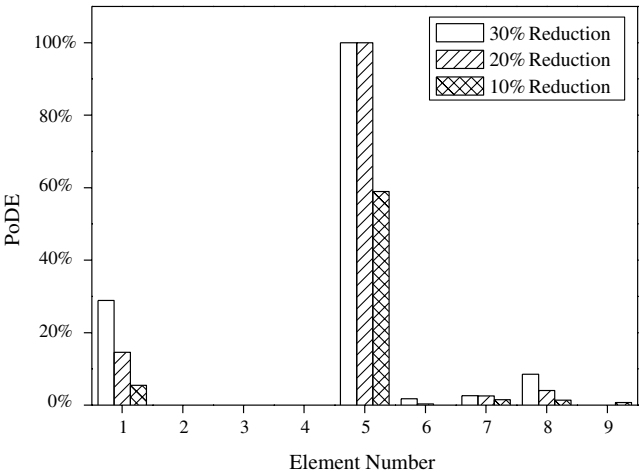

Fig. 6 PoDEs of elements at different damage levels.

values and uncertain radii of elemental stiffness parameters are obtained by the interval analysis method. Consider the case of 30% bending stiffness reduction in element 5 as an example. The mean values obtained by the interval analysis method are very close to the true value of the elemental stiffness parameters, as shown in Fig. 5. The PoDEs of each element at different damage levels are shown in Fig. 6, where element 5 is always most likely to be damaged in different cases. However, the possibility of damage in element 5 will reduce with the decrease of damage level. This is because the effect of the uncertainty level becomes larger. When the damage level of element 5 decreases to 10%, the possibility of damage in element 5 is only 55%. On the contrary, with the increase of damage level, the PoDEs of healthy elements will rise too, because the error stemming from the first-order Taylor series expansion increases with the damage level. If the damage level is too low or too high, the damaged elements may not be identified accurately or the healthy elements may be falsely identified as damaged.

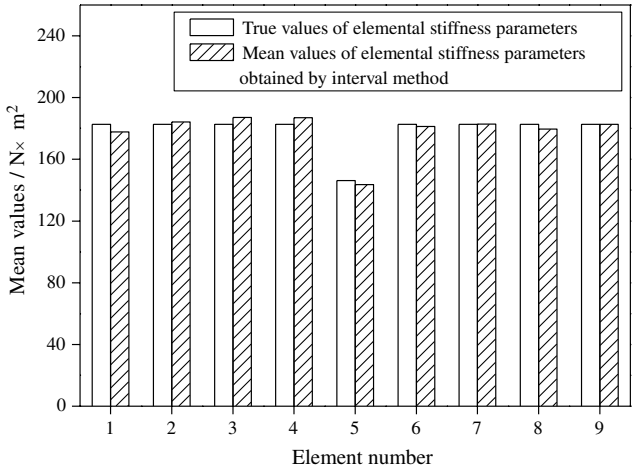

Fig. 7 Mean values of elemental stiffness parameters at the uncertainty level of 3%.

5. Study on Uncertainty Level of Natural Frequencies

The uncertainty level of measured natural frequencies seriously affects structural damage identification. If the measurement errors are too large, the true information may be submerged in noise, and the wrong identification results will be obtained. To investigate the effect of uncertainty level on the damage detection results, the numerical analyses of damage detection at different levels of uncertainty (1, 2, and 3%) in measured natural frequencies were carried out by the interval analysis method as well as Monte Carlo simulation. The damage of 20% is considered in the bending stiffness of element 5. The elemental stiffness parameter vector is obtained by the interval analysis method, and the mean values of stiffness parameters at the uncertainty level of 3% are shown in Fig. 7, which are very close to the true values. The PoDEs were then obtained and listed in Table 7 and Fig. 8. It can be seen that the PoDE of the damaged element (element 5) obtained by the interval analysis method is smaller than the PrDE obtained by the Monte Carlo Method. On the contrary, the PoDEs of healthy elements obtained by the interval method are larger than the PrDEs obtained by Monte Carlo simulation. This indicates that the present approach is an effective *nonprobabilistic* method although it is somewhat conservative. From Fig. 8, it can be seen that a higher uncertainty level leads to lower PoDEs of all the elements. In other words, the damaged element will be difficult to identify if the uncertainty level increases.

B. Example II

In this section, a steel cantilever plate with 100 elements ($m = 100$) and 121 nodes is employed to illustrate the validity of the present interval method for damage identification of structures. The FE model of the cantilever plate is shown in Fig. 9, and the

Table 7 PoDEs and PrDEs of elements at different uncertainty levels

	Interval method, PoDE, %			Monte Carlo simulation, PrDE, %		
Element number	1% uncertainty	2% uncertainty	3% uncertainty	$A_i = 0.01$	$A_i = 0.02$	$A_i = 0.03$
1	14.58	8.82	3.63	1.70	1.14	0.21
2	0.00	0.00	0.00	0.00	0.00	0.00
3	0.00	0.00	0.00	0.00	0.00	0.00
4	0.00	0.00	0.00	0.00	0.00	0.00
5	100	83.81	55.11	100	91.86	78.63
6	0.34	0.00	0.00	0.00	0.00	0.00
7	2.53	0.68	0.04	0.05	0.00	0.00
8	4.02	2.74	0.83	0.10	0.01	0.00
9	0.00	0.00	0.00	0.00	0.00	0.00

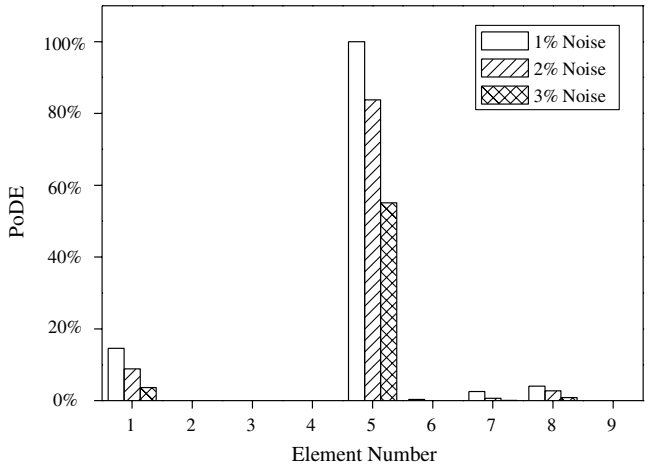

Fig. 8 PoDEs of elements at different uncertainty levels.

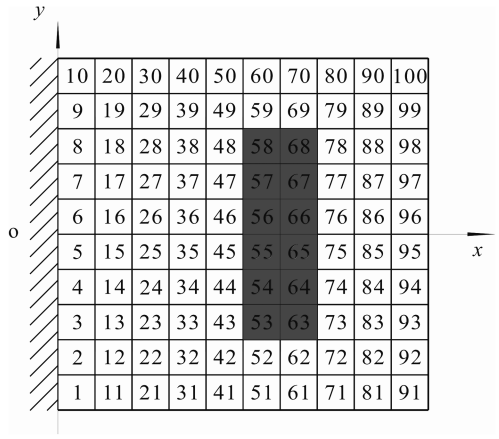

Fig. 9 FE model of the cantilever plate.

quadrilateral elements with a size of $10 \times 10 \times 1$ mm^3 are adopted. The mass density of the material is 7.5×10^3 kg/m^3. In this example, Young's modulus is considered as the elemental stiffness parameter, the Young's modulus of the initial analytical model is 1.1 times larger than that of the undamaged model, and the damaged model is the same as the undamaged model except that the Young's modulus is degraded by 30% in elements 53–58 and 63–68. As shown in Fig. 9, the shaded elements are damaged. The elemental Young's modulus of the initial model, undamaged model, and damaged model are $\alpha_{I1\text{-}100} = 2.2 \times 10^{11}$ Pa, $\alpha_{r1\text{-}100} = 2.0 \times 10^{11}$ Pa, and $\alpha_{d53\text{-}58,63\text{-}68} = 0.7 \times \alpha_{d1\text{-}52,59\text{-}62,69\text{-}100} = 1.4 \times 10^{11}$ Pa, respectively. The first 15 natural frequencies ($n = 15$) were used to detect damages in the plate, and the natural frequencies of undamaged and damaged models are assumed to be uncertain measured parameters b_i with uncertainties of 2%.

The proposed interval damage identification method was applied to detect damages in the plate. By performing the two procedures of FE model updating, the PoDEs of 100 elements were obtained and listed in Table 8. It is clear that the damaged elements have large values of PoDEs (from 87.7 to 100%). In other words, the damages were identified successfully. However, it can also be seen that some healthy elements are associated with higher PoDEs. This unintuitive fact can be explained as follows. The PoDEs of elements 52–59 and 72–79 are between 35 and 40%, the PoDEs of element 62 and element 69 equal to 58.3%. It is obvious that all of these elements lie around the damaged elements, and the stiffness reduction of damaged elements have a strong influence on these nearby healthy elements.

VII. Conclusions

In this study, the interval analysis method for structural damage identification was proposed. The measured natural frequencies in undamaged and damaged states were considered as uncertainties and described as interval numbers. Based on interval mathematics and first-order Taylor series expansion, the lower and upper bounds of the elemental stiffness parameters of the undamaged and damaged structures were obtained by the model updating method. The possibility of damage existence of each element was evaluated based on the intervals of elemental stiffness parameters in undamaged and damaged FE models. A higher value of PoDE implied a higher possibility that damage will occur. The damage identification of a steel cantilever beam and a steel cantilever plate were performed by the proposed method. Monte Carlo simulation was employed to demonstrate the validity of the present method. Through numerical examples, the interval damage identification method was illustrated to be an effective nonprobabilistic method which could deal with both single-damage and multidamage problems at different damage levels and uncertainty levels. Moreover, the generality of the present method was also illustrated: it could be applied for the damage identification of complex structures.

Table 8 Possibilities of damage existing in elements of the plate

Element number	PoDE, %	Element number	PoDE, %	Element number	PoDE, %	Element number	PoDE, %	Element number	PoDE, %
1	22.9	21	0	41	0	61	0	81	0
2	34.1	22	24.5	42	30.6	62	58.3	82	0
3	36.2	23	29.4	43	29.9	63	100	83	0
4	10.3	24	0	44	10.1	64	100	84	0
5	0	25	0	45	0	65	100	85	0
6	0	26	0	46	0	66	100	86	0
7	10.3	27	0	47	10.1	67	100	87	0
8	36.2	28	29.4	48	29.9	68	100	88	0
9	34.1	29	24.5	49	30.6	69	58.3	89	0
10	22.9	30	0	50	0	70	0	90	0
11	0	31	0	51	0	71	0	91	3.3
12	35.6	32	0	52	40.1	72	40.1	92	18.4
13	25.1	33	0	53	87.7	73	36.7	93	22
14	21.4	34	0	54	100	74	30.8	94	28.2
15	0	35	0	55	99.2	75	38.9	95	24.8
16	0	36	0	56	99.2	76	38.9	96	24.8
17	21.4	37	0	57	100	77	30.8	97	28.2
18	25.1	38	0	58	87.7	78	36.7	98	22
19	35.6	39	0	59	40.1	79	40.1	99	18.4
20	0	40	0	60	0	80	0	100	3.3

Acknowledgments

We would like to express our gratitude to Isaac Elishakoff and Tsung-Chow Su of Florida-Atlantic University and Di Yang of Georgia Institute of Technology for discussions and English improvement. We want to thank the National Science Foundation (no. 10872017), 111 Project (no. B07009), and FanZhou Science and Research Foundation for Young Scholars (no. 20080503) for financial support.

References

[1] Abo, M., "Structural Damage Detection by Natural Frequencies," *37th AIAA/ASME/ASCE/ AHS/ASC Structures, Structural Dynamics and Materials Conference and Exhibit*, AIAA, Reston, VA, 1996, pp. 1064–1069.

[2] Parloo, E., Guillaume, P., and Overmeire, M. V., "Damage Assessment Using Mode Shape Sensitivities," *Mechanical Systems and Signal Processing*, Vol. 17, No. 3, 2003, pp. 499–518. doi:10.1006/mssp.2001.1429

[3] Robinson, N. A., Peterson, L. D., and James, G. H., "Health Monitoring of Aircraft Structures Using Experimental Flexibility Matrices," *AIAA/ ASME/AHS Adaptive Structures Forum*, AIAA, Reston, VA, 1996, pp. 328–337.

[4] Yan, A., and Golinval, J. C., "Structural Damage Localization by Combining Flexibility and Stiffness Methods," *Engineering Structures*, Vol. 27, No. 12, 2005, pp. 1752–1761. doi:10.1016/j.engstruct.2005.04.017

[5] Li, C., and Smith, S. W., "Hybrid Approach for Damage Detection in Flexible Structures," *Journal of Guidance, Control, and Dynamics*, Vol. 18, No. 3, 1995, pp. 419–425. doi:10.2514/3.21404

[6] Teughels, A., Maeck, J., and Roeck, G. D., "Damage Assessment by FE Model Updating Using Damage Functions," *Computers and Structures*, Vol. 80, No. 25, 2002, pp. 1869–1879. doi:10.1016/S0045-7949(02)00217-1

[7] Jaishia, B., and Ren, W. X., "Damage Detection by Finite Element Model Updating Using Modal Flexibility Residual," *Journal of Sound and Vibration*, Vol. 290, Nos. 1–2, 2006, pp. 369–387. doi:10.1016/j.jsv.2005.04.006

[8] Cobb, R. G., and Liebst, B. S., "Structural Damage Identification Using Assigned Partial Eigenstructure," *AIAA Journal*, Vol. 35, No. 1, 1997, pp. 152–158. doi:10.2514/2.77

[9] Lim, T. W., and Kashangaki, T. A-L., "Structural Damage Detection of Space Truss Structures Using Best Achievable Eigenvectors," *AIAA Journal*, Vol. 32, No. 5, 1994, pp. 1049–1057. doi:10.2514/3.12093

[10] Elishakoff, I., "Three Versions of the Finite Element Method Based on Concepts of Either Stochasticity, Fuzziness or Anti-optimization," *Applied Mechanics Reviews*, Vol. 51, No. 3, 1998, pp. 209–218. doi:10.1115/1.3098998

[11] Collins, J. D., Hart, G. C., Hasselman, T. K., and Kennedy, B., "Statistical Identification of Structures," *AIAA Journal*, Vol. 12, No. 2, 1974, pp. 185–190. doi:10.2514/3.49190

[12] Papadopoulos, L., and Garcia, E., "Structural Damage Identification: A Probabilistic Approach," *AIAA Journal*, Vol. 36, No. 11, 1998, pp. 2137–2144. doi:10.2514/2.318

[13] Sawyer, J. P., and Rao, S. S., "Structural Fault Detection Using Fuzzy Logic," *AIAA Dynamics Specialists Conference*, AIAA, Reston, VA, 1996, pp. 214–222.

[14] Ben-Haim, Y., and Elishakoff, I., *Convex Models of Uncertainty in Applied Mechanics*, Elsevier Science, Amsterdam, 1990.

[15] Moores, R. E., *Methods and Applications of Interval Analysis*, Prentice–Hall, London, 1979.

[16] Qiu, Z. P., and Wang, X. J., "Several Solution Methods for The Generalized Complex Eigenvalue Problem with Bounded Uncertainties," *International Journal of Solids and Structures*, Vol. 42, Nos. 9–10, 2005, pp. 2883–2900. doi:10.1016/j.ijsolstr.2004.09.043

[17] Qiu, Z. P., *Convex Method Based on Non-Probabilistic Set-Theory and Its Application*, National Defence Industry Press, Beijing, 2005 (in Chinese).

[18] Qiu, Z. P., and Wang, X. J., "Comparison of Dynamic Response of Structures with Uncertain-but-Bounded Parameters Using Non-Probabilistic Interval Analysis Method and Probabilistic Approach," *International Journal of Solids and Structures*, Vol. 40, No. 20, 2003, pp. 5423–5439. doi:10.1016/S0020-7683(03)00282-8

[19] Sim, J. S., Qiu, Z. P., and Wang, X. J., "Modal Analysis of Structures with Uncertain-but-Bounded Parameters via Interval Analysis," *Journal of Sound and Vibration*, Vol. 303, Nos. 1–2, 2007, pp. 29–45. doi:10.1016/j.jsv.2006.11.038

[20] Gabriele, S., Valente, C., and Brancaleoni, F., "An Interval Uncertainty Based Method for Damage Identification," *Key Engineering Materials*, Vol. 347, 2007, pp. 551–556. doi:10.4028/www.scientific.net/KEM.347.551

[21] García, O., Vehí, J., Campos e Matos, J., Henriques, A. A., and Casas, J. R., "Structural Assessment Under Uncertain Parameters via Interval Analysis," *Journal of Computational and Applied Mathematics*, Vol. 218, No. 1, 2008, pp. 43–52. doi:10.1016/j.cam.2007.04.047

[22] Qiu, Z. P., Wang, X. J., and Ma, Y., "Comparison of Two Non-Probabilistic Methods for the Complex Eigenvalue Problem of Structures with Uncertain Parameters," *Acta Mechanica Solida Sinica*, Vol. 25, No. 3, 2004, pp. 298–304 (in Chinese).

[23] Xia, Y., and Hao, H., "Statistical Damage Identification of Structures with Frequency Changes," *Journal of Sound and Vibration*, Vol. 263, No. 4, 2003, pp. 853–870. doi:10.1016/S0022-460X(02)01077-5

[24] Hassiotis, S., and Jeong, G. D., "Identification of Stiffness Reduction Using Natural Frequencies," *Journal of Engineering Mechanics*, Vol. 121, No. 10, 1995, pp. 1106–1113. doi:10.1061/(ASCE)0733-9399(1995)121:10(1106)

A. Messac
Associate Editor